



ORIGINAL ARTICLE

Multiphoton absorption properties and bioimaging of solvent coligand cyclometalated Pt(II) complex



Jing Hu^{1,a}, Youlin Si^{1,b}, Chengkai Zhang^c, Yupeng Tian^c, Jieying Wu^c,
Junsong Yang^{a,*}

^a Teaching and Research Office of Food Safety, School of Public Course, Bengbu Medical College, Bengbu 233000, China

^b Teaching and Research Office of Analysis and Detection, School of Public Course, Bengbu Medical College, Bengbu 233000, China

^c Department of Chemistry, Anhui University, Hefei 230039, China

Received 9 March 2023; accepted 8 May 2023

Available online 15 May 2023

KEYWORDS

Cyclometalated Pt(II) complex;
Multiphoton absorption;
Solvent coligand;
Bioimaging

Abstract As a cyclometalated complex, solvent coligand Pt(II) complex with multiphoton absorption has been designed and synthesized. After the optical properties of the Pt(II) complex were studied carefully, time-dependent density functional theory calculation (TD-DFT) was used to further identify the triplet charge transitions of the complex. The specific energy levels of frontier molecular orbitals and the data related to the energy level transition showed that the Pt(II) complex had photoluminescent properties, and their phosphorescence emission originated from ³LLCT/³MLCT. Because of nonlinear optics (NLO) response, the Pt(II) complex could act as multiphoton absorption materials for bioimaging and anticancer application.

© 2023 The Author(s). Published by Elsevier B.V. on behalf of King Saud University. This is an open access article under the CC BY-NC-ND license (<http://creativecommons.org/licenses/by-nc-nd/4.0/>).

1. Introduction

Metal elements and metal complexes are ubiquitous in natural environment, and they are very important for living organisms (Elmsellem et al., 2019, M'Char et al., 2020, Bouzidi et al., 2021, Toukal et al., 2022a, Toukal et al., 2022b). The application of transition metal complexes as fluorescent probes for photodynamic therapy in bioimaging has been widely investigated (Cao et al., 2013, Fernández-Moreira

et al., 2010, Huang et al., 2015, Lo, 2020, Lv et al., 2016, Zhao et al., 2011). On the other hand, nonlinear optical (NLO) materials have been the subject of academic and commercial research for the past several decades, and a variety of NLO materials have been synthesized and studied (Goud et al., 2018, Mei et al., 2018, Zhao et al., 2018). The Pt(II) complex is particularly crucial in transition metal complexes with multiphoton absorption properties. Because it has excellent nonlinear optical response and light limiting prospect for biomedical use (Goswami et al., 2014, Zhang et al., 2013, Zhao et al., 2016). The d⁸ electronic configuration of Pt(II) complex presents a planar square structure, which brings many unique properties (Bischoff et al., 2018, Leung et al., 2016, To et al., 2013, Yam et al., 2011, Yam et al., 2015). Therefore, exploring the biological properties of Pt(II) complexes has attracted more and more scientific researchers' interest. But the premise of biological imaging is to give Pt(II) complex a certain emission behavior, which makes it glow inside living things. At the same time, Pt(II) complex has the advantage of a long phosphorescence emission lifetime. Thus, Pt(II) complexes with luminescent

* Corresponding author.

E-mail address: cacfrw@126.com (J. Yang).

¹ These authors contributed equally to this work.

Peer review under responsibility of King Saud University.



behavior and long life were designed and synthesized. Thereinto, fluorescence lifetime in living organisms is challenging. Owing to the wide application of supramolecular self-assembly lighting, supramolecular self-assembly has been intensively studied in many fields such as drug release, sensing and crystal engineering. Based on the reversibility and responsiveness of non-covalent interactions, it is of great scientific significance and practical value to use supramolecular methods to regulate molecules with special luminescence properties (Akiyoshi et al., 2018, Dong et al., 2016, Huang et al., 2015). Unlike most metal ions, Pt(II) readily forms a square coordination structure, which exhibits unique metal-metal interaction with adjacent Pt(II) centers. Such non-covalent interactions are of great interest in the field of supramolecular chemistry because the inherent tendency of this interaction is to induce groups in solution. In addition, the morphology of Pt(II) complexes nanostructures with rich spectral properties can be produced when aggregated. In recent years, platinum complexes containing pyridine (C⁺N⁻C type) have attracted extensive attention due to their excellent photoelectric properties compared with other optical materials (Puttock et al., 2018, Tashiro et al., 2018). However, most platinum complexes containing pyridine exhibit low luminescence intensity in an aqueous solution. To solve the above scientific problem, we explored forming a supramolecular self-assembly system by the intermolecular Pt...Pt stacking and π ... π interaction and displayed special luminescence properties. The Pt(II) complex with d⁸ electronic configuration coordinate form a planar square coordination configuration through open axial coordination sites.

In this study, the cyclometalated C⁺N⁻C type Pt(II) complex is designed and synthesized. When a stable M-C bond is formed between the central Pt atom and the main ligand C⁺N⁻C, the energy of the metal d orbital goes up. The NLO response of Pt(II) complex was enhanced because the ligand field effect (LF) effectively attenuates the non-radiative transition probability. The multiphoton absorption of the complex were systematically researched, and excellent properties of the Pt(II) complex for bioimaging and anticancer application were obtained.

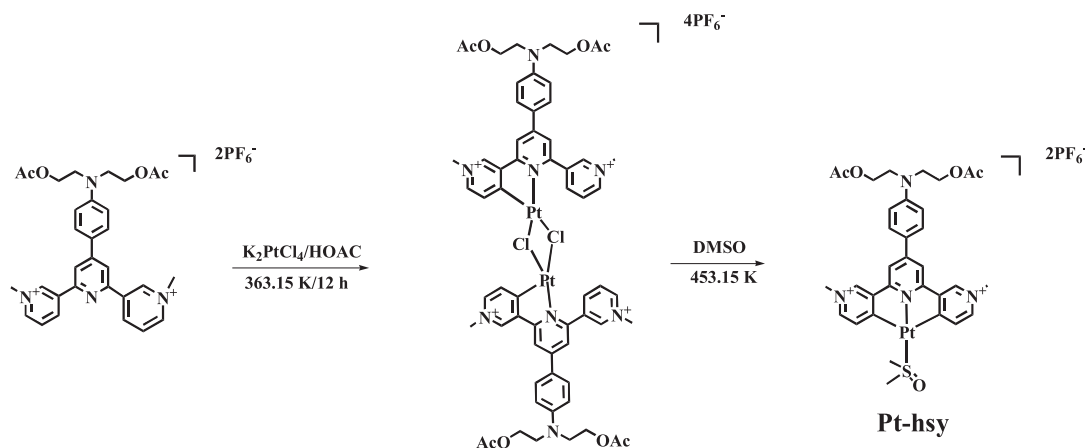
2. Materials and instruments

All chemicals were analytical reagent grade and used without further purification. In a typical preparation procedure (Scheme 1), the powder (0.41 g, 1.0 mmol) of potassium chloroplatinite added to the glacial acetic acid solution (30 mL) of the ligand hsy (0.83 g, 1.0 mmol). Thereinto, through the Solvent-free Wittig or Friedel-Crafts reactions, the ligand was synthesized in high yields and purified using recrystallization or column chromatography. The prepared

Pt(II) complex were fully characterized and their biological applications in cell imaging were investigated. Low-temperature emission test: (1) the preparation of solution 10 μ M (methyl tetrahydrofuran); (2) the use of liquid nitrogen to cool down 298 k \sim 80 k (20 K gradient); HITACHIF-7000 fluorescence spectrophotometer was used. Multiphoton absorption test: measurement system is set up, and a 1550 nm fs laser was used for multi-photon excitation (FLCPA-01C, Calmar Laser, 400 fs, 1MHz). A lens (f = 25 mm) was used to focus the laser beam onto the sample in the colorimetric cup, and the focus was near the edge of the colorimetric cup to minimize the self-absorption of the sample. The transmitted signal from the sample is collected by the objective lens (XLUMPlanFLN, 20 \times , NA = 1.00), and the objective is perpendicular to the propagation direction of the laser beam. Through a 520 nm long-pass filter, the signal is fed through the fiber into the spectrometer (PG2000, Ideoptics Instruments), and the fluorescence spectra are recorded on a computer.

3. Results and discussion

The photophysical data of Pt(II) complex(Pt-hsy) was displayed in Figure S1. The UV-absorbable spectra of the complex ranges from 200 to 600 nm. Solvents of different polarity were selected to study the effects of solvents on the absorption spectra of the complex. The sample concentration was 10 μ M, an 1 cm cuvette was used, and all solvents required for the test were chromatographic pure. The solvent had a slight influence on the position of the maximum absorption peak. As the polarity of the solvent increases, the maximum absorption peak position shift of the Pt(II) complex was less than 10 nm. It shows that the solvent molecule has no obvious effect on Pt(II) complex absorption spectra. The complex Pt-hsy has absorption peaks around 290 nm, 395 nm, and 450 nm. By discussing them, Pt(II) complex absorption spectra can effectively be attributed to Pt(II)'s ability to enhance intramolecular charge transfer (ICT). The intensity of the absorption peak decreases with the increase of solvent polarity. It shows that the interaction between solvent molecules and solute is relatively large, and the energy level difference among the complex molecules changed obviously.



Scheme 1 The synthesis routes of the complex Pt-hsy.

Due to the electron donor group (N, N-diacetate group), the absorption peak corresponding to 1MLCT (Metal To Ligand Charge Transfer) of N, N-diethyl acetate terpyridine Pt(II) complex is more evident. Increasing the length of the alkyl chain on the electron-absorbing group also causes a significant absorption peak. The above results can be explained as follows: (1) the main structure of the molecule shows excellent planarity; (2) the σ bond between the pyridine group and the phenyl group has the property of a double bond. But in solution, the σ -bond is free to rotate. The introduction of long alkyl chains reduces the molecular planarity. Therefore, the intermolecular π - π packing is weakened, which enhances intramolecular electron transfer (ICT). Time-dependent density functional theory calculation (TD-DFT) was used to identify the charge transition of platinum complex further. The theoretical calculation of the energy from the ground state of singlet to the excited state of singlet uses 6-31G* base group (C, O, H, N, S atoms) and Lanl2dz base group (Pt atoms) (Alkhamis et al., 2023, Mogharbel et al., 2023). The specific energy levels of frontier molecular orbitals are shown in Fig. 1, and the data related to the energy level transition are shown in Table 1. The HOMO of Pt(II) complex is concentrated in the central Pt atom and the orbital of the main ligand (C[^]N[^]C). The charge distribution of the central Pt atom is mainly concentrated in the $d_{x^2-y^2}$ orbital of the metal, and

the charge in the C[^]N[^]C fraction is mainly distributed in the π orbitals of the ligand. When Pt(II) complex absorbs energy, the charge transition (HOMO \rightarrow LUMO) belongs to IL[π (C[^]N[^]C) \rightarrow π^* (C[^]N[^]C)] (Abu-Dief et al., 2021, Hossan et al., 2023). The theory agrees with the experimental data, and the accuracy of the experimental data is further verified.

Time-dependent density functional theory calculation (TD-DFT) was used to further identify the triplet charge transitions of the platinum complex. The specific energy levels of frontier molecular orbitals are shown in Fig. 2, and the data related to the energy level transition are shown in Table 2. It is well-known that Pt(II) complexes have photoluminescent properties. Their phosphorescence emission originated from 3 -LLCT/ 3 MLCT. By verifying the properties of three-line emission, theoretical calculations of the lowest energy triplet of Pt(II) complex (TD-DFT) were obtained. (See Table 3.)

The home and vertical excitation energies of the first three triplet excited states (T_1 , T_2 , and T_3) are summarized in Table 2. The possible phosphorescent physical processes of Pt(II) complex are summarized in Fig. 2. The schematic energies of adiabatic energy (ΔE_{ST}) and emission energy (E_{em}) between S_0 and T_1 states of Pt(II) complex are shown in Fig. 2. The lowest energy triplet T_1 transitions give expression to from HOMO to LUMO charge, which indicate the property of 3 MLCT/ 3 LLCT and is consistent with the triplet emission

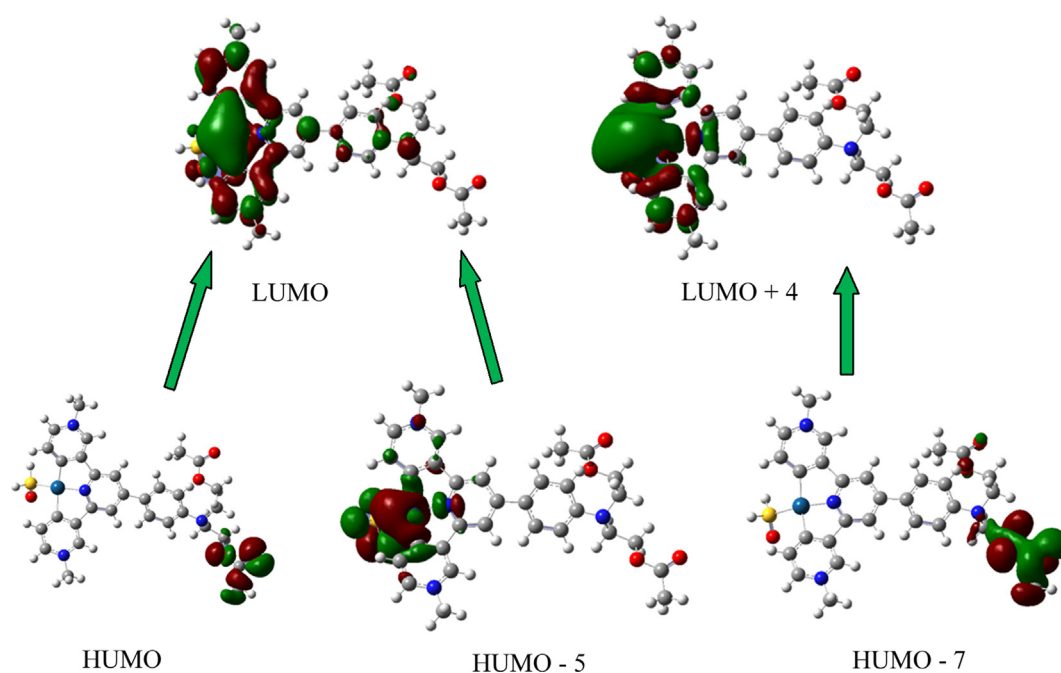


Fig. 1 The molecular orbital energy diagrams for Pt-hsy.

Table 1 The main data of the theoretical calculation for Pt-hsy.

Complex	Imax(nm)	E(eV)	Composition	Character
Pt-hsy	340	3.64	(H \rightarrow L)(0.55)	IL(π (C [^] N [^] C) \rightarrow π (C [^] N [^] C)*)
	406	3.05	(H-5 \rightarrow L)(0.15)	ICT(C [^] N [^] C)
	447	2.77	(H-7 \rightarrow L + 4)(0.55)	1 LMCT[π (C [^] N [^] C) \rightarrow d(Pt)*]mixed 1 LLCT[π (C [^] N [^] C) \rightarrow π (DMSO)*]

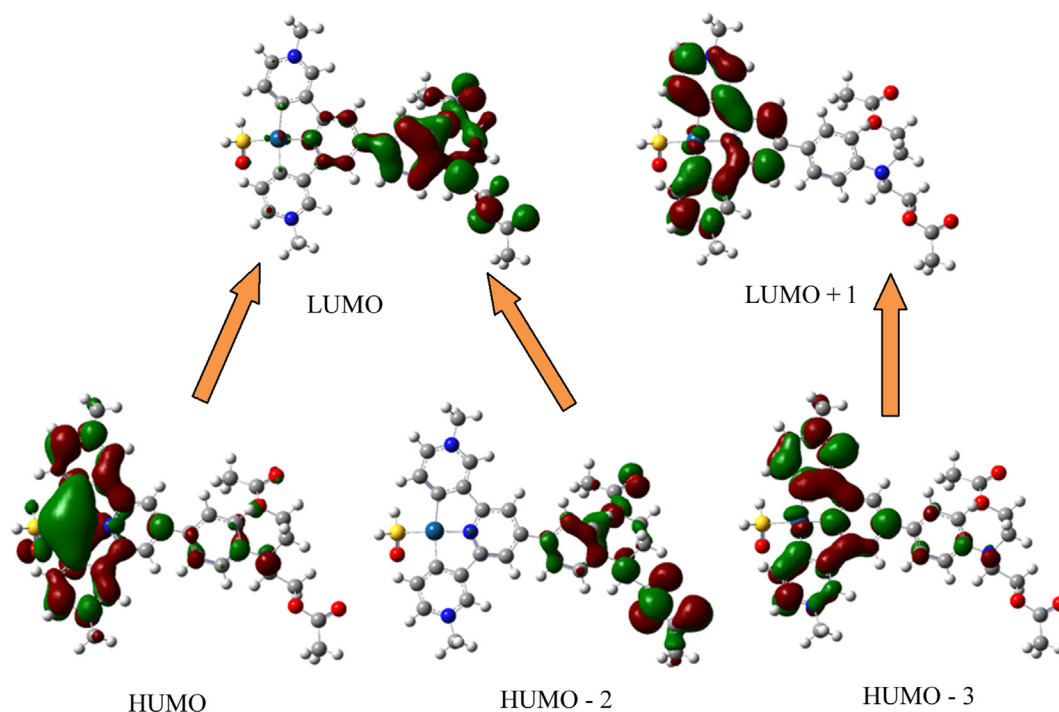


Fig. 2 The energy diagram of the triplet molecular orbitals for Pt-hsy.

Table 2 The main data of the triplet theory calculation for Pt-hsy.

Complex	State	E(eV)	Composition	Nature	Character
Pt-hsy	T ₁	2.56	H → L(0.69)	$d\pi(\text{Pt}) + \pi(\text{C}^{\wedge}\text{N}^{\wedge}\text{C}) \rightarrow \pi^*(\text{C}^{\wedge}\text{N}^{\wedge}\text{C})$	³ MLCT/ ³ LLCT
	T ₂	2.75	H-2 → L(0.54)	$\pi(\text{C}^{\wedge}\text{N}^{\wedge}\text{C}) \rightarrow \pi^*(\text{C}^{\wedge}\text{N}^{\wedge}\text{C})$	³ IL
	T ₃	3.11	H-3 → L + 1(0.53)	$d\pi(\text{Pt}) \rightarrow \pi^*(\text{C}^{\wedge}\text{N}^{\wedge}\text{C})$	³ MC

Table 3 Selected cubic NLO data for Pt-hsy at its wavelength of maximal 2PA.

Complex	λ/nm	$\beta(\text{cm}\cdot\text{GW}^{-1})$	$\sigma(\text{GM})$
Pt-hsy	780	0.068	2864

phenomenon of Pt(II) complex. The theoretical calculation is in good agreement with the experimental results.

The d-d electron transition at the lower energy level causes a non-radiative transition. Rapid non-radiative decay will result in emission quenching of the complex. Thus at low temperatures, the rotation and vibration of the molecules decrease, and low temperatures can effectively reduce the collision between molecules. The enlargement of radiative transitions probability increased the proportion of radiative transitions, and enhanced luminescence. Therefore, we tested the emission spectra of the Pt(II) complex at 298 K-80 K. The results are summarized as follows: (1) it can be seen from Fig. 3, at room temperature (298 K), the complex showed low emission intensity (Pt-hsy: $\lambda_{\text{em}} = 550 \sim 700 \text{ nm}$); (2) with the decrease of temperature (298 K – 80 K), the emission of the complex is gradually enhanced, and the emission peak is gradually refined into multiple peaks. The mechanism is that the decrease of temperature increases the viscosity of the solvent system and

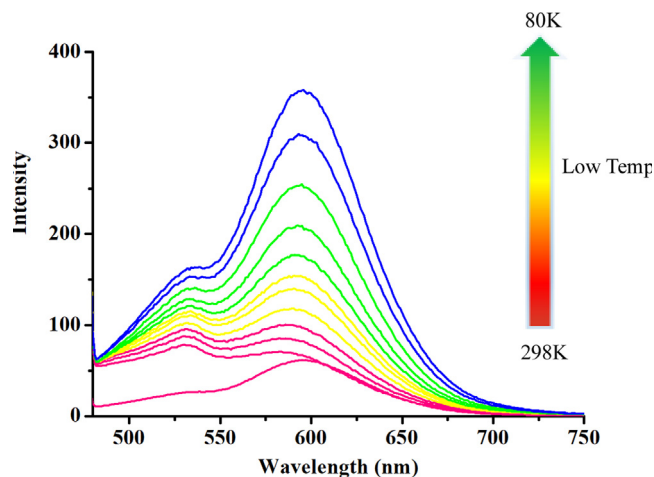


Fig. 3 The Variable-emission spectra of Pt-hsy in 2-MeTHF solution.

thus limits the rotation and vibration inside the complex. At the same time, the collision probability between solvent molecules and complexes is reduced, and the energy loss of the non-radiative transition process is reduced. As the emission intensity of the complex increases with temperature cooling, and

the emission peak gradually begins to be refined into multiple peaks. Due to the decrease in temperature, the excited molecular radiative transition becomes refined. The obvious dissipation effect of the two long alkyl chains of Pt-hsy leads to the excited state energy of the Pt(II) complex. The low-temperature emission behavior is attributed to triplet phosphorescence emission $^3\text{MLCT}[\text{d}\pi(\text{Pt}) \rightarrow \pi^*(\text{C}^*\text{N}^*\text{C})]$.

DMSO solvent was selected for the transient emission spectrum of Pt(II) complex. The sample concentration was 1 mM, and 1 cm cuvettes were used. The excitation light source is selected as 450 nm; launch window selection is 600 nm. All solvents required for the test are chromatographic pure. The transient emission spectra are shown in Figure S2.

In recent years, multiphoton absorbing materials have been paid more and more attention by researchers (Chen et al., 2017, Yokoshi and Ishihara, 2018). The mechanism of multiphoton absorption is that a designed molecule can absorb multiple photons of low energy and transition from the ground state to the excited state under felicitous conditions, then the multiphoton emission occurs. The multiphoton emission of synthesized Pt(II) complex is evident, the two-photon absorption properties of the target platinum complex were determined by the open hole Z-scan technique, including the two-photon absorption coefficient and the size of the two-photon absorption cross-section. Fig. 4 shows the open-hole fitting curve of the Pt(II) complex. First of all, the pyridine ligand has a D-A configuration. It has good two-photon absorption properties. Secondly, the coordination of metal Pt atoms can enhance the intramolecular π electron mobility of the $\text{C}^*\text{N}^*\text{C}$ type complex, thus increasing the nonlinear optical response of the Pt(II) complex. In addition, the above results indicate that Pt-hsy has excellent third-order nonlinear optical properties. It is hoped that the material will have a promising application in biology.

When a molecule absorbs three photons of low energy and transitions from the ground state to the excited state through a virtual intermediate state, back to the ground state by a radiative transition, the emission from this process is called three-photon fluorescence (Three-Photon Excited Fluorescence, 3PEF). The three-photon absorption cross section ($\delta_{3\text{PA}}$) is an important index to judge the properties of three-photon

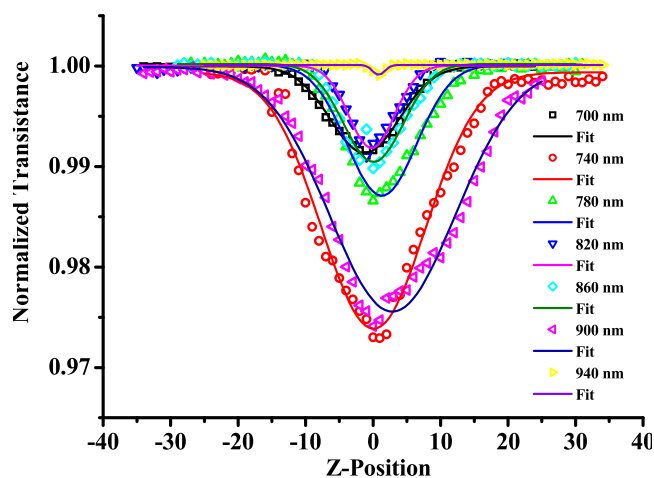


Fig. 4 The normalized open-aperture Z-scan transmittance of Pt-hsy.

materials. Combined with the triplet theory calculation, the conclusions of the variable temperature emission spectrum and transient emission spectrum are obtained.

The emission of this Pt(II) complex is attributed to triplet phosphorescence emission, and the three-photon emission behavior is also attributed to three-photon phosphorescence (3PP). Three-photon phosphorescence map (3PP) of Pt-hsy in N_2 atmosphere in the range of 1200 nm \sim 1550 nm obtained based on a laboratory multiphoton instrument (Fig. 5). The 3PP spectrum ranges from 550 nm to 650 nm, and the envelope of the spectrum is the same as that of the low-temperature emission spectrum. The peak value of Pt-hsy was obtained under 1400 nm laser excitation. It can be seen in Fig. 6 that Pt-hsy has a maximum three-photon absorption cross-section of $300 (10^{-83}\text{cm}^6\text{s}^2\text{photon}^{-2})$ at the optimal excitation wavelength. To prove that three-photon induced phosphorescence is produced, we performed three-photon validation tests on Pt(II) complex. The test results are shown in Fig. 7. The input energy and output energy are obtained by changing the power of excitation light at the maximum excitation wavelength. The results show that there is a cubic relation between the output energy and the input energy, the slope of the Pt(II) complex is around 3. Therefore, the verification result also confirmed the three-photon absorption property of the complex. It shows that the maximum absorption wavelength of two photons is 740–780 nm. Pt(II) complex can be excited by light with longer wavelengths (1400–1500 nm (NIR-II)), generating transmit signal. This 1500 nm wavelength light has a deeper transmission and penetration depth, fewer background distractions, and improved imaging clarity. Therefore, they have the potential to develop three-photon probes and be used as three-photon biological probes.

As is well-known, Pt complexes have been widely used in the field of anticancer as chemotherapy drugs for medical use, such as cisplatin, oxaliplatin, and so on. It has excellent luminescence properties, and platinum molecules with anticancer activity have attracted more and more attention from researchers. Based on the detailed study of the photophysical properties of Pt(II) complexes, the anticancer applications of $\text{C}^*\text{N}^*\text{C}$ type ring metal Pt(II) complexes will continue.

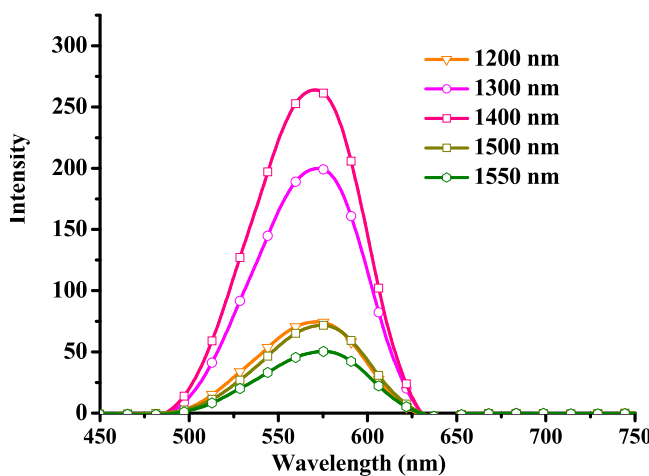


Fig. 5 The three-photon fluorescence emission spectra of Pt-hsy in DMSO solvent.

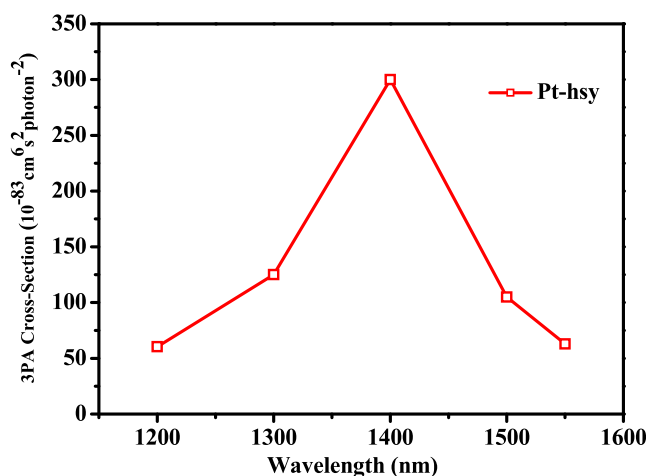


Fig. 6 The three-photon absorption cross-sections of Pt-hsy at DMSO solvent.

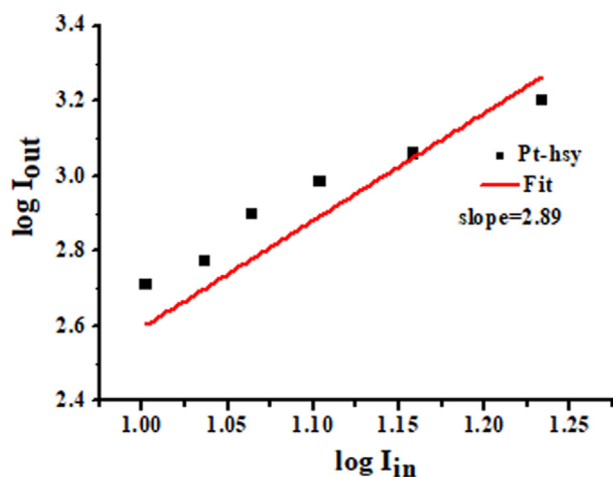


Fig. 7 The three-photon absorption verification of Pt-hsy.

MTT assay was used to determine the effect of Pt(II) complexes on HeLa (human cervical cancer cell), inhibited HeLF (mouse embryonic fibroblasts) in normal cells. Cisplatin, a commercially available anticancer drug, was selected as a contrast. To study the targeting of Pt(II) complex to the subcellu-

lar organelle, we selected HeLa cells. Subcellular organelle commercial dye lysosomes (Cell Lyso-tracker) were used for colocalization with Pt-hsy under dark conditions. The experimental results are shown in Fig. 8. Table 4 shows the IC_{50} of Pt-hsy against cancer and normal cells. The anticancer activity of the complexes against HeLa is higher than that of cisplatin ($2.5 \mu\text{M} \sim 7.5 \mu\text{M}$). In addition, it can be seen from Table 4 the complex has little damage to normal cells ($42 \mu\text{M} \sim 46 \mu\text{M}$). Compared with the toxic and side effects of traditional cisplatin, Pt-hsy has a better anticancer application prospect. Based on cytotoxicity, we investigated the subcellular organelle targeting ability of the complex. Development images were taken under the confocal microscope by adding Pt(II) complex to HeLa cells. The colocalization tracking experiment is carried out by LysoTracker and Pt-hsy. HeLa cells were co-stained by Pt-hsy ($10 \mu\text{mol/L}$) and LysoTracker ($10 \mu\text{mol/L}$), respectively. It can be seen from Fig. 11 the blue signal of the Pt(II) complex overlaps well with the red signal of the quotient dye and form a yellow signal. These results indicated that all complexes could enter the lysosomes of HeLa cells in a short time. The complexes will form vesicles by supramolecular self-assembly in phosphate buffer saline (PBS), can form nanometer vesicles with diameters over 200 nm in PBS, and can be efficiently taken up by cells. Theoretical calculation of excited states found when the complex binds to lecithin on the membrane surface of lysosomes, the electron cloud on the complex terpyridine changes significantly. Based on the above experiments, it is speculated that the mechanism of the complex targeting lysosomes is due to the formation of nanovesicles in PBS solution. When these nanovesicles enter the cell, they interact with lecithin through intermolecular forces on the surface of the lysosomal membrane. Lysosomes act as “scavengers” in the cell and are involved in the removal of damaged and aged organelles and the production of a large number of enzymes needed for cell survival, so lysosomal targeting against cancer will be more

Table 4 Inhibitory concentration IC_{50} (μM) of Pt-hsy and cisplatin.

Compound	HeLa Cells	HELF Cells
Pt-hsy	7.2 ± 0.3	52 ± 1.3
cisplatin	12.7 ± 0.8	16 ± 1.3

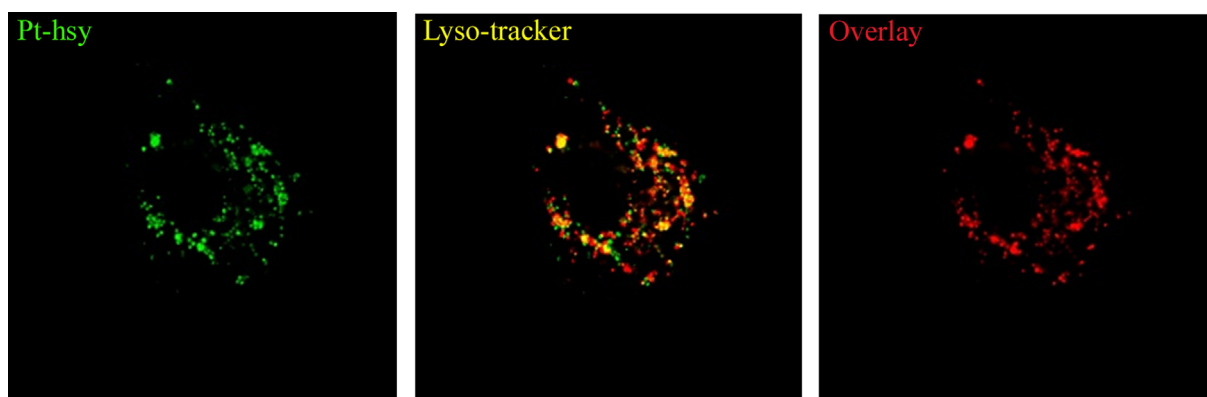


Fig. 8 Bioimaging of Pt-hsy (incubated with $10 \mu\text{M}/30 \text{ min}$ at 37°C).

accurate for high-sensitive detection (Lawrence and Zoncu, 2019, Saftig and Haas, 2016, Yu et al., 2016).

4. Conclusions

In summary, based on β -tripridine derivatives, C^NC type ring metal Pt(II) complex was obtained by forming Pt-C /N bonds. Formation conditions are gentler than the traditional Pt-C bond. The photo-physical properties of Pt(II) complexes were studied in detail. The charge transition mode of the complex was identified by theoretical calculation. At the optimal excitation wavelength, Pt(II) complex has a maximum three-photon absorption cross-section of 300 (10⁻⁸³cm⁶s²-photon⁻¹). Based on the above tests, the anticancer activity of the complex was further explored. We found the complex that had better cell-selective toxicity and subcellular organelle targeting ability (lysosome) than cisplatin, which lays the foundation for the subsequent research on anticancer mechanism.

Declaration of Competing Interest

The authors declare that they have no known competing financial interests or personal relationships that could have appeared to influence the work reported in this paper.

Acknowledgments

This work was supported by a grant for the National Natural Science Foundation of China (21271004), the Department of Education of Anhui Province (KJ2015A167); the Key Natural Science Research Foundation for University of Anhui (2022AH051442).

Appendix A. Supplementary material

Supplementary data to this article can be found online at <https://doi.org/10.1016/j.arabjc.2023.104987>.

References

- Abu-Dief, A.M., El-khatib, R.M., Aljohani, F.S., Alzahrani, S.O., Mahran, A., Khalifa, M.E., El-Metwaly, N.M., 2021. Synthesis and intensive characterization for novel Zn(II), Pd(II), Cr(III) and VO(II)-Schiff base complexes; DNA-interaction, DFT, drug-likeness and molecular docking studies. *J. Mol. Struct.* 1242, 130693.
- Akiyoshi, R., Hirota, Y., Kosumi, D., Ohtani, R., Nakamura, M., Lindoy, L.F., Hayami, S., 2018. Ferroelectric and luminescence properties of zinc(ii) and platinum(ii) soft complexes. *Dalton T.* 47 (40), 14288–14292.
- Alkhamis, K., Alatawi, N.M., Alsoliemy, A., Qurban, J., Alharbi, A., Khalifa, M.E., Zaky, R., El-Metwaly, N.M., 2023. Synthesis and Investigation of Bivalent Thiosemicarbazone Complexes: Conformational Analysis, Methyl Green DNA Binding and In-silico Studies. *Arab. J. Sci. Eng.* 48, 273–290.
- Bischoff, L., Baudequin, C., Hoarau, C., Urriolabeitia, E.P., 2018. Chapter Two - Organometallic Fluorophores of d⁸ Metals (Pd, Pt, Au). *Adv. Organomet. Chem.* 69, 73–134.
- Bouzi, A., Djedid, M., Ad, C., Benalia, M., Hafez, B., Elmsellem, H., 2021. Biosorption of Co (II) ions from aqueous solutions using selected local *Luffa cylindrica*: Adsorption and characterization studies. *Mor. J. Chem.* 9 (1), 156–167.
- Cao, R., Jia, J., Ma, X., Zhou, M., Fei, H., 2013. Membrane localized iridium(III) complex induces endoplasmic reticulum stress and mitochondria-mediated apoptosis in human cancer cells. *J. Med. Chem.* 56 (9), 3636–3644.
- Chen, W.Q., Bhaumik, S., Veldhuis, S.A., Xing, G.C., Xu, Q., Grätzel, M., Mhaisalkar, S., Mathews, N., Sum, T.C., 2017. Giant five-photon absorption from multidimensional core-shell halide perovskite colloidal nanocrystals. *Nat. Commun.* 8, 15198–15206.
- Dong, Y.W., Fan, R.Q., Chen, W., Zhang, H.J., Song, Y., Du, X., Wang, P., Wei, L.G., Yang, Y.L., 2016. Luminescence properties of a Zn(ii) supramolecular framework: easily tunable optical properties by variation of the alkyl substitution of (E)-N-(pyridine-2-ylethylidene)arylamine ligands. *RSC Adv.* 6 (111), 110422–110432.
- Elmsellem, H., Ouadi, Y.E., Mokhtari, M., Bendaif, H., Hammouti, B., 2019. A natural antioxidant and an environmentally friendly inhibitor of mild steel corrosion: a commercial oil of basil (*Ocimum basilicum* L.). *J. Chem. Technol. Metal.* 54 (4), 742–749.
- Fernández-Moreira, V., Thorp-Greenwood, F.L., Coogan, M.P., 2010. Application of d⁶ transition metal complexes in fluorescence cell imaging. *Chem. Commun.* 46, 186–202.
- Goswami, S., Wicks, G., Rebane, A., Schanze, K.S., 2014. Photo-physics and non-linear absorption of Au(i) and Pt(ii) acetylde complexes of a thienyl-carbazole chromophore. *Dalton T.* 43 (47), 17721–17728.
- Goud, N.R., Zhang, X.P., Brédas, J.L., Coropceanu, V., Matzger, A. J., 2018. Discovery of non-linear optical materials by function-based screening of multi-component solids. *Curr. For. Rep.* 4 (1), 150–161.
- Hossan, A., Aljohani, M., Alrefaei, A.F., Althumayri, K., Bayazeed, A., Saad, F.A., Abumelha, H.M., El-Metwaly, N.M., 2023. Synthesis of functionalized aminopyrazole and pyrazolopyrimidine derivatives: Molecular modeling and docking as anticancer agents. *Arab. J. Chem.* 16, 104645.
- Huang, F.H., Anslyn, E.V., 2015. Introduction: supramolecular chemistry. *Chem. Rev.* 115 (15), 6999–7000.
- Huang, H.Y., Yu, B., Zhang, P.Y., Huang, J.J., Chen, Y., Gasser, G., Ji, L.N., Chao, H., 2015. Highly charged ruthenium(II) polypyridyl complexes as lysosome-localized photosensitizers for two-photon photodynamic therapy. *Angewandte Chemie Int. Ed.* 54 (47), 14049–14052.
- Lawrence, R.E., Zoncu, R., 2019. The lysosome as a cellular centre for signalling, metabolism and quality control. *Nat. Cell Biol.* 21, 133–142.
- Leung, S.Y.L., Wong, K.M.C., Yam, V.W.W., 2016. Self-assembly of alkynylplatinum(II) terpyridine amphiphiles into nanostructures via steric control and metal–metal interactions. *P. Natl. Acad. Sci. USA* 113 (11), 2845–2850.
- Lo, K.K.W., 2020. Molecular design of bioorthogonal probes and imaging reagents derived from photofunctional transition metal complexes. *Acc. Chem. Res.* 53 (1), 32–44.
- Lv, W., Zhang, Z., Zhang, K.Y., Yang, H., Liu, S.J., Xu, A.Q., Guo, S., Zhao, Q., Huang, W., 2016. A mitochondria-targeted photosensitizer showing improved photodynamic therapy effects under hypoxia. *Angewandte Chemie Int. Ed.* 55 (34), 9947–9951.
- M'Chaar, R., Ouerfelli, N., Messaâdi, A., Zrelli, N., Ferreira, I.L., Hafez, B., Elmsellem, H., 2020. A simplified model correlating the excess properties for Bi-X binary systems (X = Cu, Sb) serving the concept of reduced Redlich-Kister function at different temperatures. *Surf. Interfaces* 21, 100643.
- Mei, D.J., Jiang, J.Q., Liang, F., Zhang, S.Y., Wu, Y.D., Sun, C.T., Xue, D.F., Lin, Z.S., 2018. Design and synthesis of a nonlinear optical material BaAl₄S₇ with a wide band gap inspired from SrB₄O₇. *J. Mater. Chem. C* 6 (11), 2684–2689.
- Mogharbel, A.T., Hossan, A., Abualnaja, M.M., Aljuhani, E., Pashameah, R., Alrefae, S.H., Abumelha, H.M., El-Metwaly, N. M., 2023. Green synthesis and characterization of new carbthioamide complexes; cyclic voltammetry and DNA/methyl green assay supported by silico ways versus DNA-polymerase. *Arab. J. Chem.* 16, 104807.
- Puttock, E.V., Walden, M.T., Williams, J.A.G., 2018. The luminescence properties of multinuclear platinum complexes. *Coordination Chem. Rev.* 367, 127–162.

- Saftig, P., Haas, A., 2016. Turn up the lysosome. *Nat. Cell Biol.* 18, 1025–1027.
- Tashiro, K., Ohtsu, H., Kawano, M., Kojima, T., Kato, T., 2018. Platinum(II) Terpyridine Complex That Switches Its Photochemical Reactivity in Response to Its Chromic Behavior in the Crystalline State. *Inorg. Chem.* 57 (21), 13079–13082.
- To, W.P., Zou, T.T., Sun, R.W.Y., Che, C.M., 2013. Light-induced catalytic and cytotoxic properties of phosphorescent transition metal compounds with a d^8 electronic configuration. *Philos. Trans. A Math. Phys. Eng. Sci.* 371 (1995), 1–19.
- Toukal, L., Belfennache, D., Foudia, M., Yekhlif, R., Benghanem, F., Hafez, B., Elmsellem, H., Abdel-Rahman, I., 2022a. Inhibitory power of N, N-(1,4-phenylene)bis(1-(4-nitrophenyl)methanimine) and the effect of the addition of potassium iodide on the corrosion inhibition of XC70 steel in HCl medium: Theoretical and experimental studies. *Int. J. Corros. Scale Inhib.* 1, 438–464.
- Toukal, L., Foudia, M., Haffar, D., Aliouane, N., Al-Noaimi, M., Bellal, Y., Elmsellem, H., Abdel-Rahman, I., 2022b. Monte Carlo simulation and electrochemical performance corrosion inhibition whid benzimidazole derivative for XC48 steel in 0.5 M H_2SO_4 and 1.0 M HCl solutions. *J. Indian Chem. Soc.* 99, 100634.
- Yam, V.W.W., Au, V.K.M., Leung, S.Y.L., 2015. Light-Emitting self-assembled materials based on d^8 and d^{10} transition metal complexes. *Chem. Rev.* 115 (15), 7589–7728.
- Yam, V.W.W., Wong, K.M.C., 2011. Luminescent metal complexes of d^6 , d^8 and d^{10} transition metal centres. *Chem. Commun. (Camb)* 47 (42), 11579–11592.
- Yokoshi, N., Ishihara, H., 2018. Giant multiphoton absorption in silicon. *Nat. Photon.* 12, 125–126.
- Yu, F.F., Chen, Z.Y., Wang, B.L., Jin, Z., Hou, Y.F., Ma, S.M., Liu, X.D., 2016. The role of lysosome in cell death regulation. *Tumor Biol.* 37, 1427–1436.
- Zhang, B.G., Li, Y.J., Liu, R., Pritchett, T.M., Haley, J.E., Sun, W.F., 2013. Extending the bandwidth of reverse saturable absorption in Platinum complexes using two-photoninitiated excited-state absorption. *ACS Appl. Mater. Interfaces* 5, 565–572.
- Zhao, Q., Huang, C.H., Li, F.Y., 2011. Phosphorescent heavy-metal complexes for bioimaging. *Chem. Soc. Rev.* 40, 2508–2524.
- Zhao, T.C., Liu, R., Shi, H., Shu, M.L., Hu, J.Y., Li, H., Zhu, H.J., 2016. Synthesis, tunable photophysics and nonlinear absorption of terpyridyl Pt(II) complexes bearing different acetylide ligands. *Dyes Pigments* 126, 165–172.
- Zhao, S.G., Yang, Y., Shen, Y.G., Wang, X.D., Ding, Q.R., Li, X.F., Li, Y.Q., Li, L.N., Lin, Z.S., Luo, J.H., 2018. A beryllium-free deep-UV nonlinear optical material $CsNaMgP_2O_7$ with honeycomb-like topological layers. *J. Mater. Chem. C* 6 (15), 3910–3916.